JOURNAL OF VIROLOGY, Apr. 2007, p. 4104–4115 Vol. 81, No. 8
0022-538X/07/$08.00+0 doi:10.1128/JVI.02681-06

Vesicular Stomatitis Viruses Resistant to the Methylase Inhibitor Sinefungin Upregulate RNA Synthesis and Reveal Mutations That Affect mRNA Cap Methylation▽

Jianrong Li,† John S. Chorba,† and Sean P. J. Whelan*

Department of Microbiology and Molecular Genetics, Harvard Medical School, 200 Longwood Ave., Boston, Massachusetts

Received 5 December 2006/Accepted 25 January 2007

Sinefungin (SIN), a natural *S*-adenosyl-L-methionine analog produced by *Streptomyces griseolus*, is a potent inhibitor of methyltransferases. We evaluated the effect of SIN on replication of vesicular stomatitis virus (VSV), a prototype of the nonsegmented negative-strand RNA viruses. The 241-kDa large polymerase (L) protein of VSV methylates viral mRNA cap structures at the guanine-N-7 (G-N-7) and ribose-2′-O (2′-O) positions. By performing transcription reactions in vitro, we show that both methylations are inhibited by SIN and that methylation was more sensitive at the G-N-7 than at 2′-O position. We further show that SIN inhibited growth of VSV in cell culture, reducing viral yield by 50-fold and diminishing plaque size. We isolated eight mutants that were resistant to SIN as judged by their growth characteristics. The SIN-resistant (SIN^R) viruses contained mutations in the *L* gene, the promoter for *L* gene expression provided by the conserved sequence elements of the *G-L* gene junction and the *M* gene. Five mutations resulted in amino acid substitutions to conserved regions II/III and VI of the L protein. For each mutant, we examined viral gene expression in cells and cap methylation in vitro. SIN^R mutants upregulated RNA synthesis in the presence of SIN, which may be responsible for their resistance. We also found that some SIN^R viruses with *L* gene mutations were defective in cap methylation in vitro, yet their methylases were less sensitive to SIN inhibition than those of the wild-type parent. These studies show that the VSV methylases are inhibited by SIN, and they define new regions of L protein that affect cap methylation. These studies also provide experimental evidence that inhibition of cap methylases is a potential strategy for development of antiviral therapeutics against nonsegmented negative-strand RNA viruses.

Vesicular stomatitis virus (VSV), the prototypic *Rhabdovirus*, has a nonsegmented negative-sense (nsNS) RNA genome of 11,161 nucleotides (nt). Infection is initiated by delivery into the host cell cytoplasm of a transcription-competent viral core (46), comprising the genomic RNA encapsidated by the nucleocapsid (N) protein and associated with the viral polymerase, a complex of the phosphoprotein (P) and the large polymerase (L) subunit (17). The genomic RNA is copied by the input polymerase to yield five capped and methylated mRNAs that encode the viral N, P, matrix (M), glycoprotein (G), and L proteins.

Our current understanding of mRNA synthesis in VSV is summarized as follows. In response to a specific promoter element (32, 49, 50), the polymerase initiates synthesis at the start sequence of the first gene (11, 51) to produce the N mRNA which is modified at its 5′ terminus to yield the cap structure $7^mGpppA^mpApCpApGpApUpApUpC$ (2). In response to a conserved gene-end sequence the polymerase polyadenylates and terminates the N mRNA (8). Termination at the end of the *N* gene is essential for polymerase to initiate synthesis at the start of the next gene, to produce the P mRNA (1, 5). The mRNAs are not synthesized in equimolar quantities (48); rather, their abundance decreases with the distance between the gene and the 3′ promoter. This gradient of transcription reflects a poorly understood transcriptional attenuation event that is localized to the gene junction regions (27). The 241-kDa L protein contains the active site for ribonucleotide polymerization (44) and is responsible for cotranscriptional formation of the 5′-mRNA cap structure (21–23, 30, 31) and 3′-poly(A) tail (25). Although the total number of the genes can vary, this strategy for gene expression is shared by all viruses in the families *Rhabdoviridae*, *Filoviridae*, and *Paramyxoviridae*.

The 5′-mRNA cap structure is formed by a series of enzymatic reactions, each of which are distinct to those employed by the host. Specifically, for VSV the 5′ pppApApCpApG must be modified to remove two phosphates to yield a 5′ pApApCpApG which is capped by transfer of GDP to yield the G*ppp*ApApCpApG cap structure (2). This contrasts with cellular capping in which an RNA triphosphatase removes a single phosphate and an RNA guanylyltransferase transfers GMP. The mRNA cap structure is then methylated by methyltransferases (MTases) at both guanine-N-7 (G-N-7) and ribose-2′-O (2′-O) positions to yield the $7^mGpppA^mpApCpApG$ cap structure (33). For VSV the two MTase activities use a single binding site for the methyl donor *S*-adenosyl-L-methionine (SAM) (31). In contrast, host mRNA cap structures are methylated by two separate enzymes, first at the G-N-7 position and then at the 2′-O position. Although best characterized for VSV, the unusual capping reactions are conserved among the nsNS RNA viruses, with the notable exception that some

* Corresponding author. Mailing address: Harvard Medical School, Department of Microbiology and Molecular Genetics, 200 Longwood Ave., Boston, MA 02115. Phone: (617) 432-1923. Fax: (617) 738-7664. E-mail: swhelan@hms.harvard.edu.

† These authors contributed equally to this study.

▽ Published ahead of print on 14 February 2007.

Paramyxovirus family members produce mRNAs that lack a 2′-O methyl group (12).

Capping enzymes of many viruses are attractive candidates for chemotherapeutic intervention, and the methylation enzymes are no exception (13). In this regard, many adenosine analogues have been shown to inhibit the replication of a range of viruses in cell culture and diminish pathogenesis in small animal models (15). A proposed mechanism of inhibition mediated by such adenosine analogues is through interference with the host enzyme *S*-adenosyl homocysteine (SAH) hydrolase. SAH hydrolase is critical for converting SAH, the byproduct of SAM-dependent MTases, into homocysteine and adenosine, and the products of this reaction are inhibitory to SAH hydrolase. Adenosine analogues such as 3-deazaeplanocin-A are potent antiviral agents, and previous work has shown a correlation between the ability of such analogues to inhibit SAH hydrolase and VSV replication in cell culture (14).

Sinefungin (SIN) is a natural adenosine analog produced by *Streptomyces griseolus* and a known potent inhibitor of MTases. SIN is structurally related to SAM, except the methyl group that is donated from SAM is replaced by an amino group in SIN. Crystal structures of several MTases have been solved in complex with SIN (42, 43, 52), which binds to a region that overlaps the SAM binding site. SIN has been shown to have both antiviral and antifungal properties (18, 35, 37, 41, 52). Specifically, SIN was shown to inhibit the MTases of Newcastle disease virus (NDV) and vaccinia virus in vitro, as well as vaccinia virus plaque formation on L cells (41). While these experiments demonstrated that viral cap methylation reactions are inhibited by SIN, resistant mutants were not isolated. In addition, NDV mRNAs are not 2′-O methylated (12); thus, the effects of SIN on both cap methylations have not been previously described for an nsNS RNA virus.

In this report, we show that SIN inhibits the VSV MTases in vitro, demonstrating that the viral L protein can serve as a direct target of SIN inhibition. We also show that SIN inhibits viral growth in cell culture, and we further isolate SIN-resistant (SIN^R) mutants. These mutants increased RNA synthesis in the presence of SIN, suggesting that upregulation of viral gene expression can lead to resistance. Sequence analysis of the genomes of resistant mutants identified previously unrecognized regions of the *L* gene that can impact mRNA cap methylation. These studies thus show that the inhibition of cap methylation enzymes of VSV can be used as a strategy to inhibit viral growth, and they suggest a means by which the virus can become resistant to such inhibition.

MATERIALS AND METHODS

Isolation of SIN^R viruses. Vero cells were pretreated with the indicated concentration of SIN (Sigma Chemical Co., St Louis, MO) in exogenous medium for 1 h prior to infection with recombinant VSV (rVSV) at a multiplicity of infection (MOI) of 0.1. Infection was performed in the presence of 2.56 mM SIN, the cell culture fluids were collected at 20 h postinoculation (hpi), and the viral titer was determined by plaque assay. SIN^R mutants were selected by repeated virus passage in the presence of SIN as follows. Cells were pretreated with 2.56 mM SIN for 1 h and infected with rVSV at an MOI of 0.01. Individual plaques were isolated at 36 hpi and used to seed cells for amplification of virus. Virus was subjected to three further rounds of growth in the presence of 2.56 mM SIN except that cells were inoculated at an MOI of 0.1, and the cell culture fluids were collected when a significant cytopathic effect was visualized by microscopy. The plaque diameter of these passaged variants was measured in the presence and absence of 2.56 mM SIN to identify mutants that exhibited a growth advantage over the rVSV parent. To confirm that these variants were resistant to SIN, cells were infected at an MOI of 3.0, and the yield of virus was determined at 24 hpi in the presence and absence of SIN.

Identification of the SIN^R mutations. The entire genome of the selected mutants was sequenced. Viral particles were isolated by incubation of the supernatant with IE-2 anti-VSV-G monoclonal antibody (kindly provided by Isabella Novella) for 1 h at 37°C, and the complex was isolated on protein G-linked magnetic beads (New England BioLabs, Beverly, MA). Genomic viral RNA was extracted using the RNAeasy kit (QIAGEN), and nine overlapping fragments that span the entire genome were produced by reverse transcription-PCR (RT-PCR) using a one-step RT-PCR kit (QIAGEN). The PCR products were purified and subsequently sequenced at the DF/HCC DNA Sequencing Facility, Harvard Medical School. The sequences of the leader and trailer regions were determined following RNA ligation using T4 RNA ligase (New England Biolabs, Beverly, MA) and RT-PCR across the ligated junction. PCR products were cloned into pGEMT (Promega, Madison, WI) prior to sequence determination. Mutations were identified by alignment with the rVSV sequence using DNAstar software. Large stocks of the SIN^R mutants were generated by inoculation of 8 to 10 confluent T150 flasks of BHK-21 cells at an MOI of 0.01. The viral titer was determined by plaque assay on Vero cells, and the protein content was measured by use of Bradford reagent (Sigma Chemical Co.). The entire genome of the purified viruses was sequenced again, and these stocks were used for in vitro transcription reactions.

Single-cycle growth curves. Confluent BHK cells were infected with individual viruses at an MOI of 3. After 1 h of adsorption, the inoculum was removed, cells were washed with Dulbecco's minimal essential medium (DMEM), fresh DMEM (supplemented with 2% fetal bovine serum) was added, and infected cells were incubated at 37°C. Aliquots of the cell culture fluid were removed at the indicated intervals, and the viral titer was determined by plaque assay on Vero cells.

Analysis of gene expression in cells. At the indicated time postinoculation, BHK-21 cells were incubated with DMEM containing 10 $\mu g\ ml^{-1}$ actinomycin-D (act-D). Following 1 h of incubation, the medium was replaced with fresh medium containing act-D and [^{3}H]uridine (30 $\mu Ci\ ml^{-1}$) (Perkin Elmer, Wellesley, MA). At the indicated time postlabeling, a cytoplasmic extract was prepared, and RNA was purified following phenol and chloroform extraction as described previously (38). Purified RNA was analyzed by electrophoresis on acid-agarose gels (29) and detected by fluorography.

For protein synthesis, at the indicated time postinoculation, cells were washed with methionine- and cysteine-free medium and incubated with fresh medium supplemented with act-D (10 $\mu g\ ml^{-1}$). Following 1 h of incubation, the medium was replaced with free medium supplemented with EasyTag [^{35}S]-Express (40 $\mu Ci\ ml^{-1}$) (Perkin Elmer). Cytoplasmic extracts were prepared and analyzed by sodium dodecyl sulfate-polyacrylamide gel electrophoresis (SDS-PAGE). Labeled proteins were detected either by autoradiography or by using a phosphorimager.

Transcription of viral RNA in vitro. Viral RNA was synthesized in vitro as described previously (6), with minor modifications (51). Purified rVSV (20 μg) was activated by incubation with detergent for 5 min at room temperature. RNA synthesis reactions were performed in the presence of nucleoside triphosphates (1 mM ATP and 0.5 mM each of CTP, GTP, UTP) and 25% (vol/vol) rabbit reticulocyte lysate, which provides additional SAM in the reaction. Where indicated, reaction mixtures were supplemented with 20 μM SAM or SAH or 15 μCi of [α-^{32}P]GTP (3,000 $Ci\ mmol^{-1}$).

Cap MTase assay. To examine the extent of cap methylation, purified RNAs were digested with one or more of the following: nuclease P1 (Sigma), tobacco acid pyrophosphatase (TAP; Epicenter, Madison, WI), RNase T_2 (Invitrogen), and alkaline phosphatase (New England BioLabs). To examine G-N-7 methylation, in vitro transcription reactions were performed in the presence of [α-^{32}P]GTP and 20 μM SAM or SAH. To examine 2′-O methylation, in vitro transcription reactions were performed in the presence of 20 μM [^{3}H]SAM. Products of RNA synthesis were purified and digested with the appropriate cocktail of nucleases, and the products were analyzed by thin-layer chromatography (TLC) on polyethyleneimine-F (PEI-F) cellulose sheets (EM Biosciences). Plates were developed using 1.2 M LiCl and dried, and the spots were visualized using a phosphorimager. The markers 7^mGpppA and GpppA (New England Biolabs, Beverly, MA) and their TAP digestion products were visualized by UV shadowing at 254 nm.

Primer extension assays. A negative-sense oligonucleotide corresponding to nucleotides 130 to 115 of the complete VSV genome sequence was end-labeled using [γ-^{32}P]ATP and T4 polynucleotide kinase (Invitrogen, Carlsbad, CA). The labeled primer was purified away from unincorporated nucleotide using a QIAquick nucleotide removal kit (QIAGEN, Valencia, CA). Labeled primer

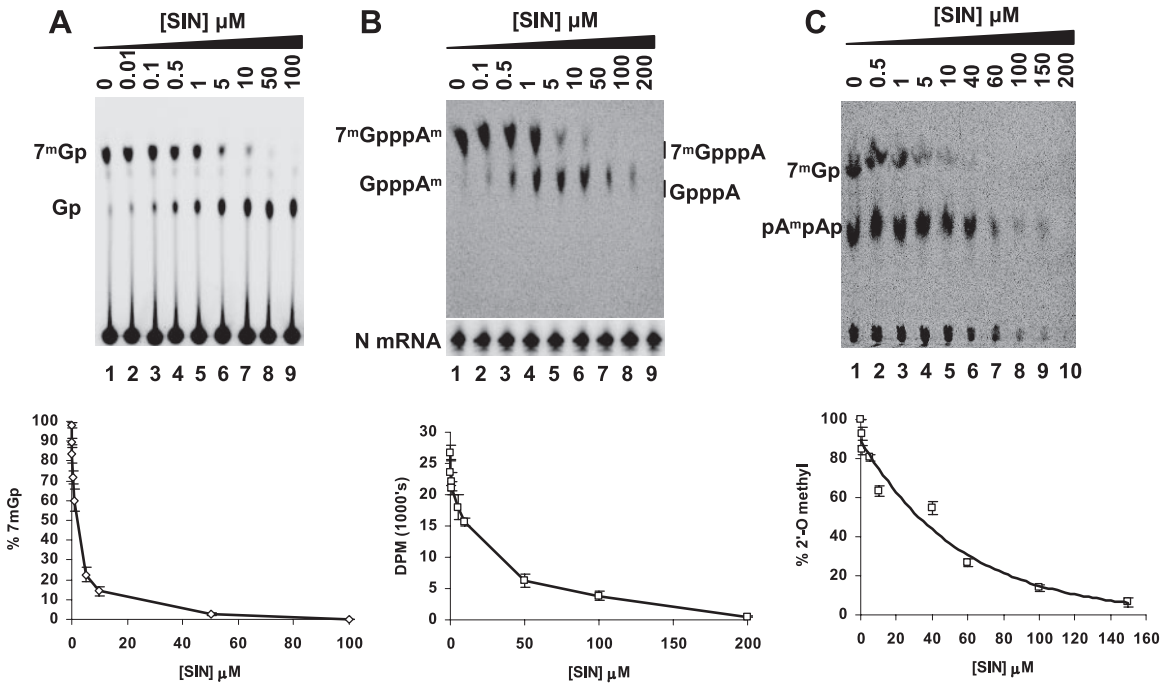

FIG. 1. SIN inhibits VSV mRNA cap methylation in vitro. (A) G-N-7 methylation. Viral mRNA was synthesized in vitro in the presence of the indicated concentration of SIN and 15 μCi [α^{32}P]GTP. The products were purified, digested with 2 units of TAP, and subjected to TLC on PEI-F cellulose sheets. The plates were dried, and the spots were visualized using a phosphorimager. The migration of the markers 7^{m}Gp and Gp is shown. Quantitative analysis of results from three independent experiments was used to generate the graph shown (bottom), from which an IC_{50} for SIN inhibition was calculated. (B) Cap methylation. (Top) RNA was synthesized in the presence of [^{3}H]SAM and the indicated concentration of SIN, and the products were purified and digested with nuclease P1 prior to TLC on PEI-F cellulose sheets. The plates were dried, and the spots were visualized by phosphorimage analysis. The migration of the 7^{m}GpppA and GpppA markers is shown. (Middle) RNA from the top panel was examined by primer extension using a primer designed to anneal to the N mRNA. (Bottom) Quantitative analysis of results from three independent experiments was used to generate the graph shown, from which an IC_{50} for SIN was calculated. (C) 2′-O methylation. (Top) RNAs produced as described for panel B were hydrolyzed with TAP and RNase T_2 prior to TLC analysis. The migration of the 7^{m}Gp marker is shown, and the presumed pA^{m}pAp spot is identified. (Bottom) Quantitative analysis used to calculate the IC_{50} for 2′-O methylation.

(0.2 pmol) was annealed with one-twenty-fifth of the total RNA from an in vitro transcription reaction and extended by Superscript III reverse transcriptase (Invitrogen) at 50°C. Products were analyzed by electrophoresis on denaturing 6% polyacrylamide gels and detected by phosphorimage analysis.

Quantitative analysis. Quantitative analysis was performed using a phosphorimager (GE Healthcare, Typhoon) and ImageQuant TL software (GE Healthcare, Piscataway, NJ). Statistical analysis was performed on results from three to five separate experiments, and the calculated means along with the standard deviation are shown in each figure. The significance of the values was determined using a paired Student's *t* test.

RESULTS

SIN inhibits VSV mRNA cap methylation in vitro. SIN, a natural nucleoside analog isolated from *Streptomyces griseolus*, is a structural analog of SAM and a potent inhibitor of MTases. We examined whether SIN could function as an inhibitor of the VSV MTases by measuring the effect of increasing concentrations of SIN on mRNA methylation. Briefly, 20 μg of purified VSV was activated with detergent and incubated with nucleoside triphosphates supplemented with [α^{32}P]GTP and 20 μM SAM in the presence of increasing concentrations of SIN. RNA was extracted and purified as described, and the extent of G-N-7 methylation was determined by hydrolysis of the mRNA cap structure with TAP, followed by TLC on PEI-F cellulose sheets. TAP specifically cleaves the pyrophosphate bond of the GpppApApCpApG cap structure to yield Gp or, if the cap structure is methylated, 7^{m}Gp. For rVSV, when transcription reactions were performed in the presence of 20 μM SAM, a single product of TAP cleavage was detected (Fig. 1A, lane 1). This product comigrated with a 7^{m}Gp marker and not the Gp marker, generated by TAP cleavage of 7^{m}GpppA and GpppA, respectively, and thus showed that for VSV the cap structure was fully G-N-7 methylated. Inclusion of SIN in the transcription reactions led to a dose-dependent inhibition of G-N-7 methylation (Fig. 1A, lanes 2 to 9) such that at 50 μM SIN, G-N-7 methylation was negligible (Fig. 1A, lane 8). Quantitative analysis of three independent experiments was used to calculate a 50% inhibitory concentration (IC_{50}) of 2.5 μM SIN for G-N-7 methylation (Fig. 1A, bottom).

To examine the effect of SIN on 2′-O methylation, transcription reactions were performed in vitro in the presence of 20 μM [^{3}H]SAM. RNA was purified and digested with nuclease P1 prior to analysis by TLC on PEI-F cellulose sheets as described in Materials and Methods. Nuclease P1 cleaves the bond between the 3′-hydroxyl group and the 5′-phosphoryl group of adjacent nucleosides. Thus, cleavage of VSV mRNAs by P1 could yield 7^{m}GpppA^{m}, GpppA^{m}, 7^{m}GpppA, or GpppA, depending on the extent of mRNA cap methylation. For rVSV, a single product of P1 cleavage was observed, consistent with the fully methylated cap structure 7^{m}GpppA^{m} (Fig. 1B, lane 1). Inclusion of SIN in the transcription reactions led to a dose-

dependent inhibition of both G-N-7 and 2′-O methylation (Fig. 1B, lanes 2 to 9). However, the two methylations were differentially sensitive to SIN inhibition, as shown by the accumulation of the GpppA^m form of the cap structure at 1 to 100 μM SIN (Fig. 1B, lanes 4 to 8). Thus, 2′-O methylation was less sensitive than G-N-7 methylation to SIN inhibition. Consistent with the data shown in Fig. 1A, the IC_{50} for the G-N-7 MTase was calculated as 2.5 μM SIN. To confirm that approximately equal quantities of RNA were synthesized in vitro in the presence of SIN, the samples used for nuclease P1 digestion were examined by primer extension assay. Irrespective of the quantity of SIN added to the in vitro reaction mixture, approximately equal amounts of an 80-nt product that corresponded precisely to the 5′ end of the N mRNA were observed (Fig. 1B, middle). The IC_{50} for 2′-O methylation was estimated by measuring the total quantity of incorporated [^{3}H]SAM by scintillation counting of the RNA. In the absence of SIN, the cap structure was fully double methylated, which corresponds to approximately 27,000 dpm. Half of this, or 13,500 dpm, was attributed to methylation at the 2′-O position. At concentrations above 10 μM SIN, G-N-7 methylation was negligible (Fig. 1A, bottom). An IC_{50} for 2′-O methylation can thus be extrapolated from the concentration of SIN that corresponds to 6,250 dpm (Fig. 1B, bottom), which is approximately 40 μM.

To directly measure the IC_{50} for 2′-O methylation the [^{3}H]SAM-labeled RNAs were hydrolyzed by use of RNase T_2 and TAP. RNase T_2 is an endoribonuclease that cleaves preferentially 3′ of A residues, but the phosphodiester bond is resistant to cleavage if the ribose is 2′-O methylated. Digestion of the VSV cap structure 7^{m}GpppA^{m}pApCpApG with RNase T_2 should yield 7^{m}GpppA^{m}pAp if the cap structure were fully methylated, and TAP would digest this to yield 7^{m}Gp, pA^{m}pAp, and Pi. Consistent with this, treatment of the [^{3}H]SAM-labeled RNAs with TAP and T_2 yielded two products, one that comigrated with the 7^{m}Gp marker and one that was consistent with pA^{m}pAp (Fig. 1C, lane 1). Increasing the concentration of SIN from 0.5 to 200 μM diminished both G-N-7 and 2′-O methylation, with G-N-7 being more sensitive than 2′-O (Fig. 1C, top). Quantitative analysis showed that the IC_{50} for G-N-7 methylation was 2.5 μM. To determine the IC_{50} for 2′-O methylation, the amount of pA^{m}pAp was plotted versus the concentration of SIN (Fig. 1C, bottom). This yielded an IC_{50} of 32 μM for SIN inhibition of 2′-O methylation. These data thus demonstrate that the two VSV methylase activities are sensitive to SIN inhibition, and they show that G-N-7 methylation was more sensitive than the 2′-O methylation.

Effect of SIN on the replication of VSV. Given that SIN functioned as an inhibitor of VSV mRNA cap methylation in vitro, we examined its ability to inhibit virus replication in cell culture. Briefly, rVSV was used to infect BHK cells (MOI = 3) that were pretreated with increasing amounts of SIN. The titer of virus was determined by plaque assay on Vero cells, and the results are depicted in Fig. 2A. The viral yield was reduced in a dose-dependent manner, with an approximate IC_{50} of 220 μM. To demonstrate that the effect on virus replication was not simply a consequence of toxicity of SIN to cells, we evaluated cell viability by trypan blue exclusion. Following 24 h of incubation, SIN concentrations of up to 5.12 mM had no significant effect on cell viability (Fig. 2A). Higher concentrations of SIN resulted in cell toxicity, with only 63% of the cells being viable at 7.68 mM

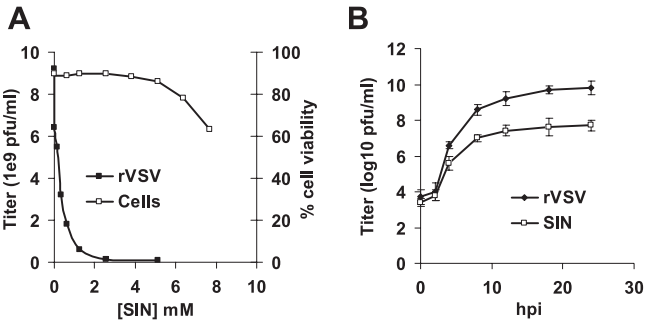

FIG. 2. SIN inhibits VSV replication in BHK cells in culture. (A) BHK cells were inoculated with VSV at an MOI of 3 in the presence of the indicated [SIN], and the viral yield was determined by plaque assay at 24 hpi. The titer of virus is plotted against the dose of SIN to generate the curve shown. Cell viability was monitored by determining the percentage of uninfected cells that excluded trypan blue following 24 h of incubation with the indicated [SIN]. (B) Single-step growth assay. BHK cells were infected with VSV at an MOI of 3 in the presence or absence of 2.56 mM SIN, and the viral titer was determined at the indicated times postinoculation.

SIN (Fig. 2A). These experiments thus show that viral replication was more sensitive to SIN inhibition than cell viability.

To examine in more detail the effects of SIN on the kinetics of viral replication, a single-step growth assay was performed with wild-type VSV in the presence and absence of SIN. Growth of VSV in the presence of 2.56 mM SIN added to the exogenous medium resulted in a 50-fold reduction in virus yield as determined by plaque assay (Fig. 2B). This difference was statistically significant as judged by a paired Student's *t* test ($P < 0.05$). These experiments thus show that SIN inhibits the growth of VSV in cell culture.

Selection of viral mutants that exhibit resistance to SIN. The quasispecies nature of RNA virus populations suggested that it might be possible to select for viral mutants that were resistant to the effects of SIN on viral growth. Consequently, virus was serially amplified in the presence of 2.56 mM SIN. Following four passages, the ability of viruses to replicate in the presence and absence of SIN was examined by measuring the diameter of 50 viral plaques (Fig. 3A) and also by determining the viral titer at 24 hpi (Fig. 3B). For rVSV, SIN significantly diminished viral plaque diameter from 4.2 ± 0.5 mm to 3.3 ± 0.5 mm at 36 hpi ($P < 0.05$). Eight viruses that showed resistance, as judged by the relative plaque diameter in the presence of SIN, were isolated (Fig. 3A). In the absence of SIN, the plaque diameter of these mutants was reduced compared to that of rVSV, ranging from 1.2 ± 0.4 mm for SIN^R mutant 7 (SIN^{R}7) to 3.4 ± 0.4 mm for SIN^{R}1. However, in the presence of SIN, the plaque diameter was not significantly altered ($P > 0.05$). Consistent with the effect of SIN on viral plaque diameter, the viral mutants were also resistant to SIN inhibition as judged by their titers (Fig. 3B). At 24 hpi, rVSV titers were diminished by 50-fold, whereas the mutants showed a modest two- to threefold reduction in viral yield (Fig. 3B). These data thus confirm that the growth of these viruses in cell culture was resistant to SIN inhibition.

SIN^{R}1 accumulated to slightly elevated titers compared with rVSV, whereas titers of each of the other mutants were similar or modestly reduced. We thus performed a single-step growth

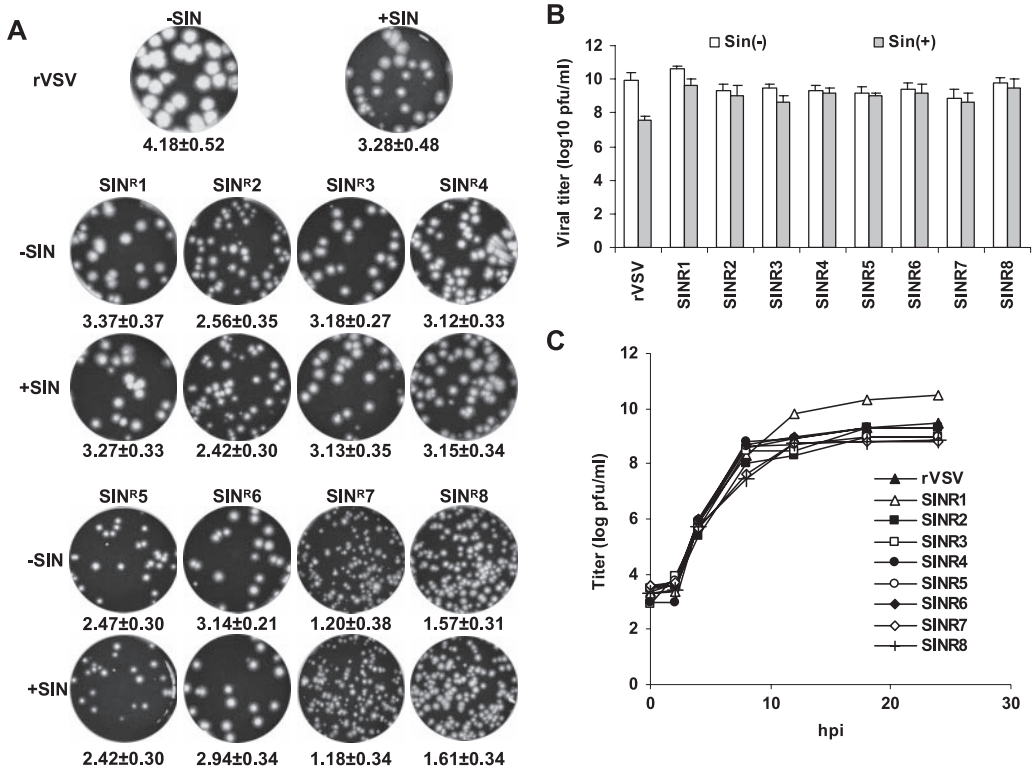

FIG. 3. Growth properties of SIN^R mutants. (A) Plaque morphologies of rVSV and each of the SIN^R mutants in the presence or absence of 2.56 mM SIN on Vero cells at 36 hpi is shown. The identity of the virus is indicated above the plaques, and the mean diameter (in millimeters ± standard deviation) is shown below. (B) Effect of SIN on viral yield. BHK cells were inoculated with each of the indicated viruses at an MOI of 3 in the presence or absence of 2.56 mM SIN, and the viral yield was determined at 24 hpi. (C) Single-step growth assay. BHK cells were infected with virus at an MOI of 3, and the viral titer was determined at the indicated times postinoculation.

assay for each of the mutants in the absence of SIN (Fig. 3C). These experiments confirmed that SIN^{R}1 grew to elevated titers compared with rVSV and demonstrated that differences in the replication kinetics of the other SIN^R mutants were modest (Fig. 3C).

Sequence analysis of resistant viruses. To identify the changes associated with resistance to SIN, the entire genome of each SIN^R mutant was amplified by RT-PCR. The sequence of the resulting cDNA was determined and compared to that of pVSV1(+), the rVSV parent. The majority of mutations were within the *L* gene and its promoter provided by the conserved sequences at the *G-L* gene junction. For five viruses, SIN^{R}2, -4, -5, -7, and -8, these mutations resulted in amino acid changes to conserved regions (CR) II/III and VI of the L protein (Table

TABLE 1. Summary of phenotypic properties of SIN^R mutants

Virus	Mutation	Consequence	% Methylation[a]		Avg fold increase in presence of SIN[b]		
			7 mG	2′ mA	mRNA	Protein	Genome
rVSV			97	100	1.1	1.0	1.1
SIN^{R}1	U2413C	D55G in M protein	96	100	1.7–3.1	1.0–2.8	3.2
	U insertion at position 4721	G gene end expanded to U8					
SIN^{R}2	U9678G	K1749T in L protein (CR VI)	30	30	2.3–3.8	1.0–2.7	2.0
	U insertion at position 4721	G gene end expanded to U8					
SIN^{R}3	U insertion at position 4721	G gene end expanded to U8	95	100	1.8–2.7	1.0–1.5	1.5
SIN^{R}4	G6200A	P490S in L protein (CR II)	96	100	1.5–2.2	1.0–2.3	1.5
SIN^{R}5	A6255G	M498T in L protein (CR II)	80	83	1.0–1.4	0.9–1.4	1.6
SIN^{R}6	C4728A	C5A in L gene start sequence	85	88	1.4–1.9	0.9–1.6	1.6
SIN^{R}7	A2401C	M51R in M protein	38	33	2.6–4.4	0.9–2.4	4.4
	A6531G	I600T in L protein (CR III)					
SIN^{R}8	U2413C	D55G in M protein	42	42	1.0–1.5	0.8–2.0	1.6
	C6755U	G675R in L protein (CR III)					

[a] 7 mG, guanine-N-7 methylation; 2′ mA, ribose 2′-O methylation.
[b] mRNA, protein, and genome levels are expressed as the relative amounts observed in cells in the presence of SIN versus the absence of SIN. For mRNA and protein levels, expression of the N, P, M, G, and L genes varied in the range provided. The absolute amounts are plotted in Fig. 7C (mRNA) and Fig. 8B (protein).

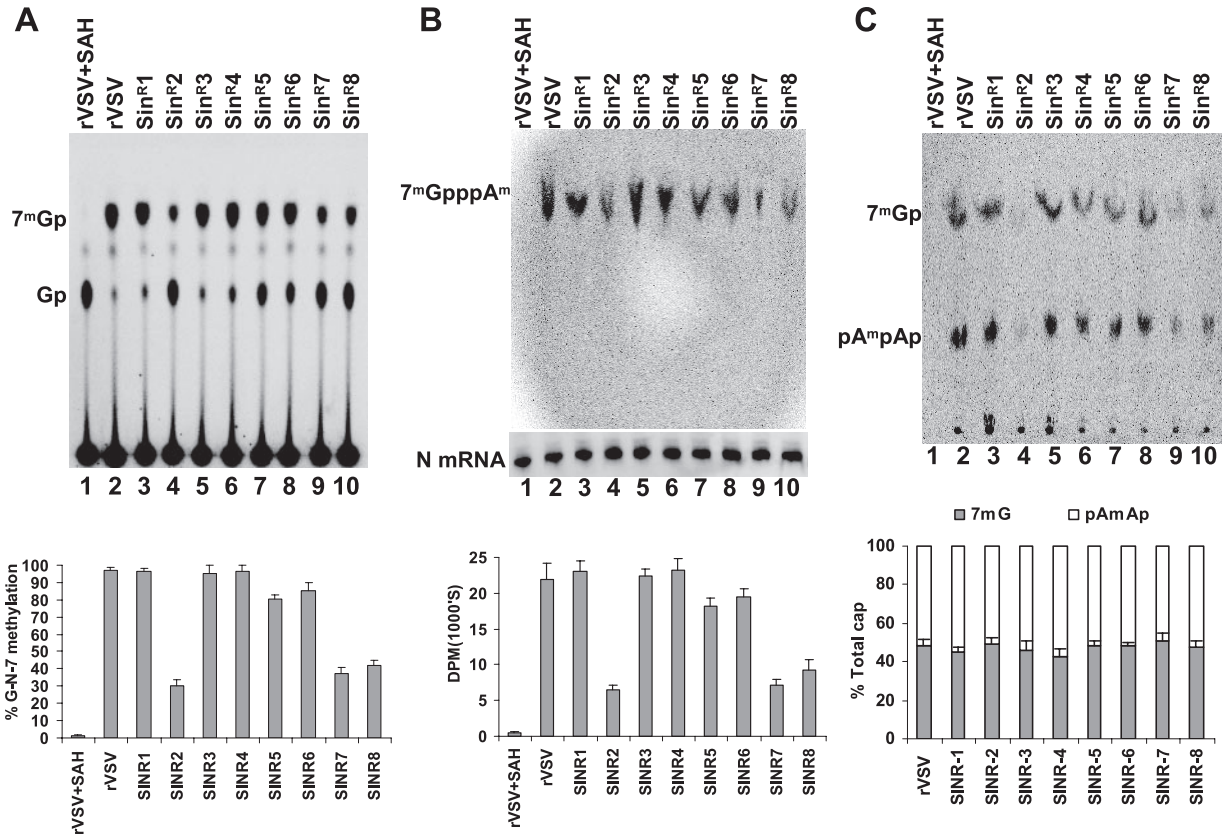

FIG. 4. Effect of SIN^R mutations on cap methylation in vitro. (A) G-N-7 methylation. (Top) Viral mRNA was synthesized in vitro in the presence of 15 μCi [α^{32}P]GTP. The products were purified, digested with 2 units of TAP, and subjected to TLC on PEI-F cellulose sheets. The plates were dried, and the spots were visualized using a phosphorimager. The migration of the markers 7^{m}Gp and Gp is shown. (Bottom) Quantitative analysis of results from three independent experiments was used to generate the graph shown. (B) Cap methylation. (Top) RNA was synthesized in the presence of [^{3}H]SAM, and the products were purified and digested with nuclease P1 prior to TLC on PEI-F cellulose sheets. The plates were dried, and the spots were visualized by phosphorimage analysis. (Middle) RNA from the top panel was examined by primer extension using a primer designed to anneal to the N mRNA. (Bottom) Quantitative analysis of results from three independent experiments was used to generate the graph shown. (C) 2′-O methylation. RNAs produced as described for panel B were hydrolyzed with TAP and RNase T_2 prior to TLC analysis. The migration of the 7^{m}Gp marker is shown, and the presumed pA^{m}pAp spot is identified. (Bottom) The ratio of G-N-7 and 2′-O methylation is shown.

1). In addition, mutants SIN^{R}1 and -8 contained a mutation in the *M* gene which resulted in the amino acid change D55G. Mutant SIN^{R}7 also contained a mutation in the *M* gene that resulted in the amino acid change M51R.

SIN^R mutants exhibit defects in mRNA cap methylation. We and others previously reported that CR VI of the VSV L protein functions as an mRNA cap MTase (21, 22, 30, 31). We generated amino acid substitutions to the predicted catalytic and SAM binding residues and showed that several of these substitutions resulted in the total inhibition of mRNA cap methylation in vitro. These recombinant viruses exhibited growth defects in cell culture, but remarkably some substitutions diminished viral yield by only 1 log compared to rVSV. These experiments showed that defects in cap methylation were not lethal to VSV, and so we evaluated the extent of cap methylation of each SIN^R mutant. Large stocks of virus were generated by amplification in the absence of SIN, the virus was purified, and the sequence was confirmed. RNA was synthesized in vitro in the presence of [α^{32}P]GTP and 20 μM SAM and purified as described, and the extent of G-N-7 methylation was determined by hydrolysis of the cap structure with TAP followed by TLC. For rVSV, when transcription reactions were performed in the presence of 20 μM SAH, a single product of TAP cleavage was detected (Fig. 4A, lane 1) that comigrated with the Gp marker. When reactions were carried out in the presence of SAM the product of TAP cleavage comigrated with the 7^{m}Gp marker, demonstrating that the cap structure was fully G-N-7 methylated (Fig. 4A, lane 2). By contrast, five of the SIN^R mutants, SIN^{R}2 and -5 to -8, showed defects in G-N-7 methylation (Fig. 4A, lanes 4 and 7 to 10, respectively). These defects ranged from a modest 15% reduction in G-N-7 for SIN^{R}6 to a 70% reduction for SIN^{R}2 (Fig. 4A, bottom).

To determine whether the SIN^R mutants were defective in 2′-O methylation, transcription reactions were performed in vitro in the presence of 20 μM [^{3}H]SAM. RNA was purified and digested with nuclease P1 prior to analysis by TLC on PEI-F cellulose sheets. For rVSV, a single product of P1 cleavage was observed, consistent with the fully methylated cap structure 7^{m}GpppA^m (Fig. 4B, lane 2). Each of the SIN^R mutants synthesized some fully methylated cap (Fig. 4B, lanes 3 to 10); however, the abundance of the methylated cap structure was diminished for SIN^{R}2 and -5 to -8. To demonstrate

that this decrease in the amount of the double methylated cap structure was not due to a reduction in mRNA synthesis, the quantity of N mRNA in each sample was examined by primer extension assay. For each virus an 80-nt product was detected, which corresponds to the 5′ end of the N mRNA, and quantitative analysis showed that the levels were indistinguishable for each of the SIN^R viruses (Fig. 4B, middle). To determine the total extent of mRNA cap methylation, the amount of [^{3}H] transferred to the mRNAs was measured by scintillation counting, and the number of dpm was normalized to the amount of RNA synthesized by each virus (Fig. 4B, bottom). These data showed that the total extent of methylation was diminished for mutants SIN^{R}2 and -5 to -8.

To demonstrate that both methylations were inhibited for SIN^{R}2 and -5 to -8, RNAs synthesized in the presence of [^{3}H]SAM were purified and hydrolyzed with TAP and RNase T_2 as described previously (30, 31). For rVSV and each of the SIN^R mutants, both 7^{m}Gp and pA^{m}pAp products were detected (Fig. 4C, lanes 2 to 10). While the absolute abundances of the 7^{m}Gp and pA^{m}pAp products varied between mutants, quantitative analysis of the ratio of the two products obtained from three independent experiments was 1:1 (Fig. 4C, bottom). This is consistent with both G-N-7 and 2′-O methylation being reduced to the same extent for SIN^{R}2 and -5 to -8.

Effect of SIN on cap methylation by SIN^R mutants. While some of the SIN^R mutants were defective in cap methylation, we hypothesized that the methylation might be more resistant to SIN. To test this, we performed in vitro transcription reactions in the presence of 0 to 200 μM SIN. To examine G-N-7 methylation, reactions were carried out in the presence of [α^{32}P]GTP, 20 μM SAM, and the indicated [SIN]. The RNA was purified as described, the cap structure was hydrolyzed with TAP, and the products were analyzed by TLC on PEI-F cellulose sheets (Fig. 5A). These data confirmed that SIN^{R}2 and -5 to -8 are defective in G-N-7 methylation compared to rVSV (Fig. 5A). Quantitative analysis (Fig. 5B) showed that G-N-7 methylation was more resistant to SIN inhibition for some mutants. At 2 μM SIN, which is close to the IC_{50} for G-N-7 methylation, approximately 55% G-N-7 methylation was seen for rVSV. In contrast, mutants SIN^{R}2, -4, -7, and -8 showed elevated levels of G-N-7 methylation, yielding 85% ± 4%, 78% ± 5%, 69% ± 3%, and 68% ± 3% 7^{m}Gp, respectively. Levels of 7^{m}Gp were not significantly different between SIN^{R}2 and SIN^{R}4 at 2 μM SIN ($P > 0.05$). However, at 50 μM SIN, SIN^{R}4 was clearly more resistant, showing 17% ± 3% compared to 5% ± 1% 7mGp for SIN^{R}2 (Fig. 5B). To show that each of the SIN^R mutants synthesized equal amounts of RNA in vitro in the presence of SIN, we examined the RNA products on acid-agarose urea gels as described previously (29, 30). These data confirmed that even at 50 μM SIN, which was the highest concentration used in the in vitro synthesis reactions, the products were unaltered (Fig. 5C). These data thus showed that for SIN^{R}2, -4, -7, and -8, G-N-7 methylation was less sensitive to SIN inhibition than it was for rVSV.

To examine 2′-O methylation, reactions were performed in the presence of [^{3}H]SAM and the indicated [SIN]. The RNA was purified as described, the cap structure was hydrolyzed with nuclease P1, and the products were analyzed by TLC on PEI-F cellulose sheets (Fig. 6A). Each SIN^R mutant synthesized equal amounts of mRNA in vitro in the presence of SIN

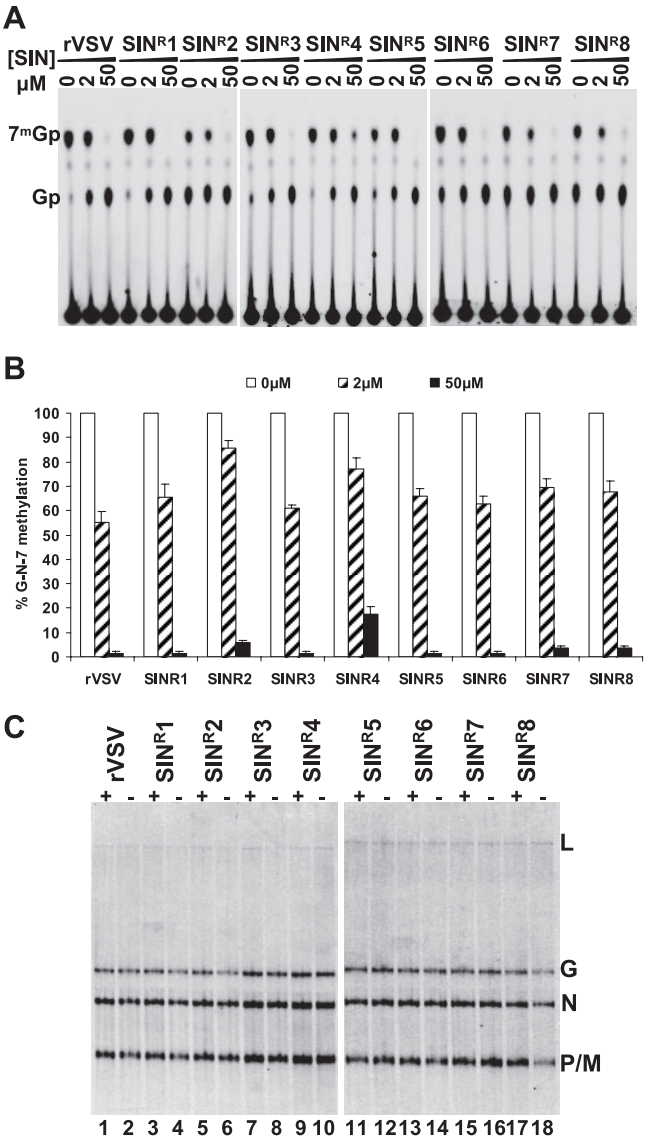

FIG. 5. Effect of SIN on SIN^R G-N-7 methylation in vitro. (A) TLC analysis of the TAP cleavage products of mRNA synthesized in the presence of different concentrations of SIN. An autoradiograph of the TLC plate is shown, and the virus and the concentration of SIN are indicated. The migration of 7^{m}Gp and Gp markers are shown. (B) Quantitative analysis of results from three independent experiments was used to generate the graph shown. (C) SIN does not affect viral RNA synthesis in vitro. RNAs were synthesized in vitro in the presence of 50 μM SIN and analyzed on acid-agarose gels as described in the text.

as shown by measuring N mRNA levels by primer extension (Fig. 6B). Quantitative analysis of the methylated cap structures (Fig. 6C) showed that methylation was more resistant to SIN inhibition for some mutants. In the presence of 200 μM SIN, SIN^{R}4 was the most resistant, showing 25% ± 2% 2′-O methylation. Levels of 2′-O methylation were undetectable for all other viruses at 200 μM SIN. In addition, the 2′-O methylase activities of mutants SIN^{R}2, -7, and -8 showed more modest levels of resistance to SIN, possessing 58% ± 6%, 47% ± 4%, and 49% ± 5% 2′-O methylase activity at 50 μM SIN,

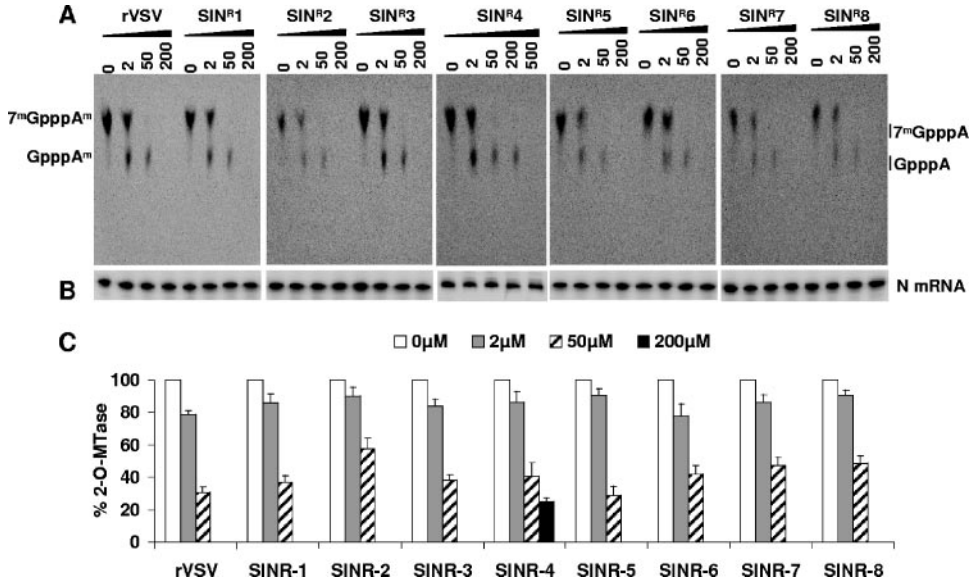

FIG. 6. Effect of SIN on SIN^R 2′-O methylation. (A) RNAs were synthesized in vitro in the presence of [^{3}H]SAM and the indicated concentration of SIN. RNAs were hydrolyzed with nuclease P1 and analyzed by TLC. The migration of 7^{m}GpppA and GpppA reference markers is shown, and the 7^{m}GpppA^m and GpppA^m products are identified. (B) Primer extension analysis on N mRNA was performed as described in Materials and Methods. (C) Quantitative analysis of the effect of SIN on the extent of 2′-O methylation. For each mutant, the amount of 2′-O methylation in the absence of SIN was set at 100%.

respectively. This compares with 30% ± 3% for rVSV (Fig. 6C). These data thus show that both the G-N-7 and 2′-O MTases of some SIN^R mutants are more resistant to SIN inhibition than those of rVSV.

SIN leads to increased gene expression for the SIN^R mutants. The experiments described above showed that several SIN^R mutants were defective in cap methylation but that these methylations were less sensitive to SIN inhibition than those of rVSV. We anticipated that this might be accompanied by a change in gene expression in cells that might account for the growth properties of the SIN^R mutants. To test this we examined viral RNA and protein synthesis in infected cells.

To examine RNA synthesis, BHK-21 cells were infected with either rVSV or the SIN^R mutants at an MOI of 3, and RNA was metabolically labeled from 4 to 7 hpi by incorporation of [^{3}H]uridine in the presence of act-D and, where indicated, 2.56 mM SIN. Total cytoplasmic RNA was extracted, purified, and analyzed by electrophoresis on acid-agarose urea gels (Fig. 7A). Quantitative analysis of three independent experiments showed that SIN^R mutants had a significant increase in the abundance of the replication products in the presence of SIN. The amount of genomic RNA was increased 1.5- to 4.4-fold for each mutant in the presence of SIN compared to the absence of SIN, and these were significantly different ($P < 0.05$) from the 1.1-fold alteration observed for rVSV (Fig. 7B and Table 1). Consistent with this increase in template abundance, the levels of mRNA were typically increased in the presence of SIN (Fig. 7C and Table 1). In comparison to rVSV, SIN^{R}7 synthesized less RNA (Fig. 7B and C), but treatment of cells with SIN led to an increase in RNA synthesis by this mutant (Table 1). Only one mutant, SIN^{R}5, did not show a significant increase in levels of mRNA, despite the increase in template abundance (Fig. 7C and Table 1). Beyond an overall increase in RNA levels in the presence of SIN, no other property was shared by all SIN^R mutants. For some mutants a readthrough transcript containing G and L is clearly evident between the L and V RNAs (Fig. 7A). Although the abundance of this transcript varies, this transcript is often seen for rVSV and does not correlate with the presence of any specific mutation.

To examine protein synthesis, BHK-21 cells were infected with either rVSV or the indicated SIN^R mutant at an MOI of 3, and proteins were labeled by metabolic incorporation of [^{35}S]methionine from 4 to 7 hpi in the presence or absence of SIN. Total cytoplasmic proteins were analyzed by SDS-PAGE and detected by phosphorimage analysis (Fig. 8A). Quantitative analysis of results from three independent experiments showed that the levels of N protein were relatively unchanged for each of the mutants, even in the presence of SIN (Fig. 8B). Mutants SIN^{R}2 and -5 to -8 all synthesized less L protein than rVSV did in the absence of SIN. Four of these mutants, SIN^{R}2, -5, -7, and -8, contained amino acid changes in L (Table 1), suggesting that these alterations might destabilize L. Intriguingly, mutant SIN^{R}6 contained a single nucleotide change within the *L* gene start (Table 1) and produced wild-type levels of L mRNA (Fig. 7C), suggesting that this mRNA was not efficiently translated. The levels of other viral proteins varied, such that increased levels of protein were seen for several of the SIN^R mutants in the presence of SIN (Fig. 8 and Table 1). The most consistent increases were seen for G protein, which was elevated 1.4- to 2.2-fold, and for L protein, which, with the exception of SIN^{R}5, was elevated 1.3- to 2.8-fold in the presence of SIN. While variations were seen for the P and M proteins, these tended to be of smaller magnitude and were not universal. These data show that the SIN-resistant viruses typically increased viral protein synthesis in the presence of SIN,

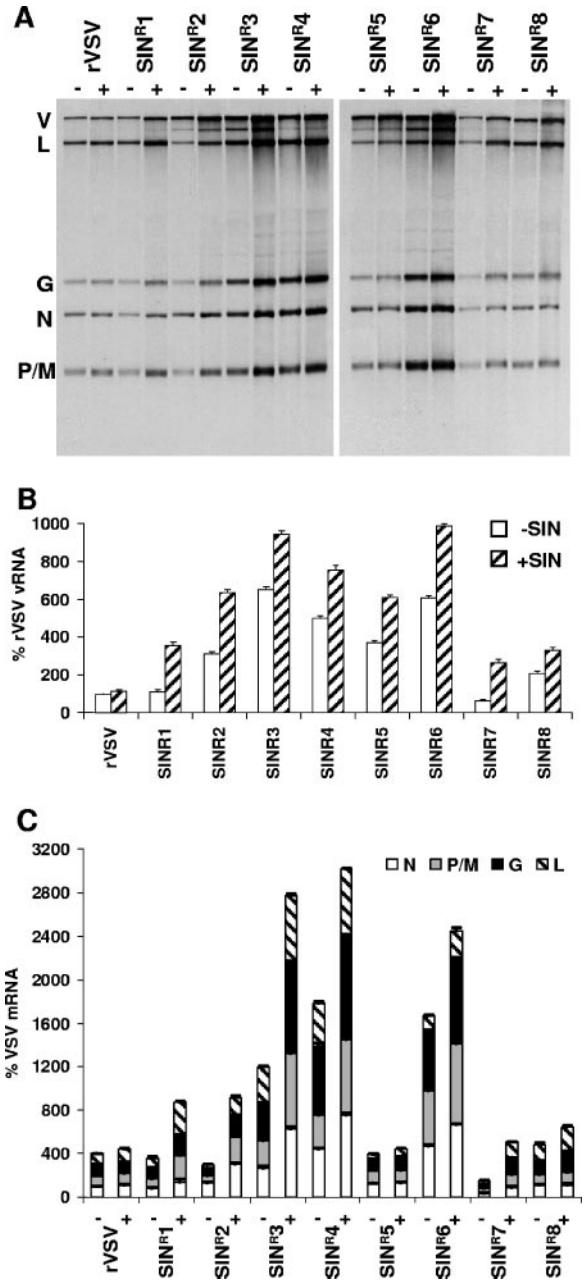

FIG. 7. Viral RNA synthesis in BHK cells. (A) Cells were pretreated with SIN and infected at an MOI of 3, and RNAs were labeled by incorporation of [^{3}H]uridine in the presence of act-D from 4 to 7 hpi as described in the text. Total cytoplasmic RNA was extracted, resolved by electrophoresis on acid-agarose gels, and visualized by fluorography. RNA extracted from an equivalent number of cells was loaded in each lane. The SIN^R virus and the identity of the viral RNA species are indicated as follows: V, genomic and antigenomic replication products; L, G, N, and P/M, mRNA. Note that the P and M mRNAs comigrate on these gels. (B and C) Quantitative analysis of the effect of SIN on viral RNA. (B) Replication products. (C) mRNAs. The abundance of V RNA and each individual mRNA are expressed relative to those obtained for rVSV in the absence of SIN, and these values were set at 100% such that the total level of mRNA products for rVSV was equal to 400%.

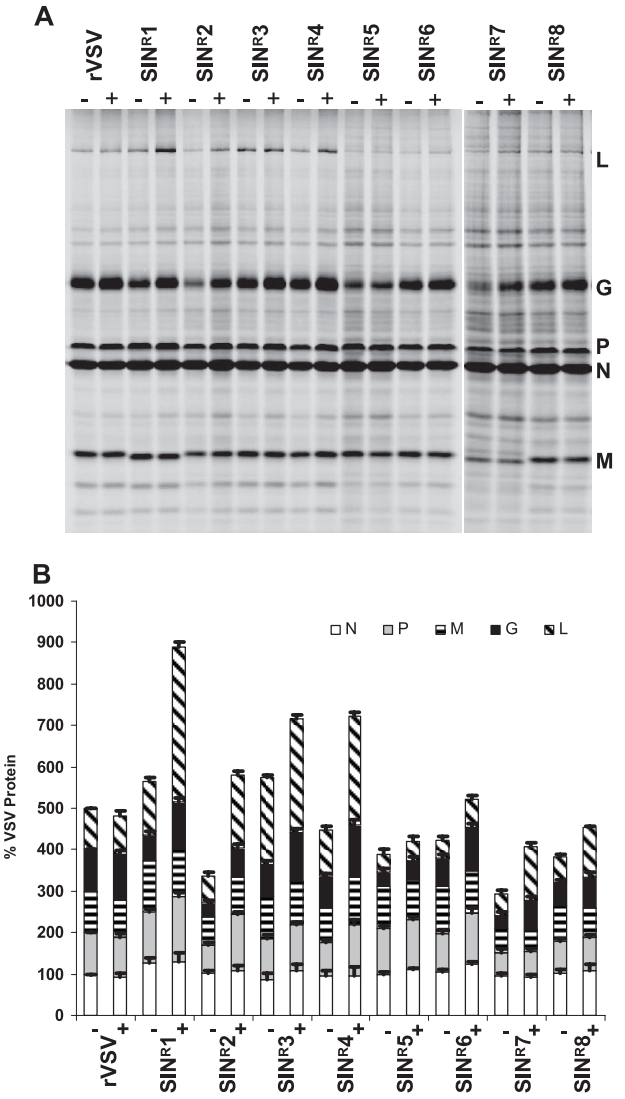

FIG. 8. Viral protein synthesis in BHK cells. (A) Cells were pretreated with SIN and infected at an MOI of 3, and proteins were labeled by incorporation of [^{35}S]methionine-cysteine in the presence of act-D from 4 to 7 hpi as described in the text. Cytoplasmic extracts were prepared, and proteins were resolved by SDS-PAGE and detected using a phosphorimager. Extract from an equivalent number of cells was loaded in each lane. The SIN^R virus and the identity of the viral proteins are shown. (B) Quantitative analysis of results from three independent experiments. Bar graph showing each of the viral proteins represented by the indicated shading as a percentage of protein compared to that synthesized by rVSV in the absence of SIN. Levels of each protein were set at 100% for rVSV in the absence of SIN, yielding a total of 500%.

suggesting that increased gene expression may lead to SIN resistance.

DISCUSSION

We selected eight VSV mutants that were resistant to the known MTase inhibitor SIN and characterized the properties of these mutants with regard to growth and gene expression in cells and RNA synthesis and mRNA cap formation in vitro.

The mutations detected in the SIN^R mutants were within the *L* gene or its promoter element provided by the conserved 23-nt sequence of the *G-L* gene junction or within the *M* gene. All SIN^R mutants synthesized higher levels of viral RNA in cells in the presence of SIN than in the absence of SIN (Fig. 7B). This was often accompanied by an increase in viral mRNA and protein production and likely led to the mutants having an advantage over the rVSV parent for growth in the presence of SIN. Several mutants exhibited defects in mRNA cap methylation in vitro that were accompanied by single-amino-acid substitutions in conserved regions II/III and VI of the L protein or by a mutation to the conserved gene start sequence. These methylations were less sensitive to SIN inhibition, demonstrating that these mutations decreased the ability of SIN to interfere with methylation. These experiments directly demonstrate that both VSV MTases are sensitive to SIN inhibition, they suggest a means by which the virus can acquire resistance to this inhibitor, they reveal new regions of L protein that can impact mRNA cap methylation, and they suggest that components of the gene start sequence can influence mRNA cap methylation.

Viral and cellular targets of SIN inhibition. The X-ray crystal structures of several MTases have been solved in complex with SIN (42, 43, 52). In each of these structures, the binding site of SIN overlaps that for SAM and SAH, demonstrating that SIN can directly target these MTases. The MTase activities of VSV reside within the *L* gene (23), and genetic and biochemical evidence suggests that both G-N-7 and 2′-O methylase activities use a single binding site for SAM (31). The K_m for SAM for 2′-O methylation is 0.2 μM, whereas that for G-N-7 methylation is 10 μM (47). In the present report, we have shown that both VSV MTase activities were inhibited by SIN in vitro and that G-N-7 methylation was more sensitive than 2′-O methylation, with IC_{50} values of 2.5 and 32 μM, respectively. These data are consistent with SIN directly binding the L protein at the SAM binding site and inhibiting its MTase activities. Viral mRNA capping enzymes have been proposed as attractive targets for the development of chemotherapeutics (13), and these data support the hypothesis that SIN can directly target the viral mRNA cap methylation enzymes of VSV in vitro.

Previous work with the paramyxovirus NDV showed that the IC_{50} for SIN inhibition of G-N-7 methylation was 150 nM (41). This contrasts with the IC_{50} of 2.5 μM reported here for VSV G-N-7 methylation. This may reflect a differential sensitivity of VSV over NDV to SIN inhibition, but it could also reflect the different sources of SIN used in these experiments. In addition, SIN concentrations of 25 μM were toxic to L cells in culture (41), which markedly contrasts with the 2.56 mM SIN used in the present study with BHK and Vero cells (Fig. 2A). Whether this difference in cell toxicity reflects different sources of SIN, its chemical stability, or cellular uptake is unknown. Despite these differences our data show that SIN inhibits VSV replication and that in vitro the viral MTases are targets of SIN inhibition.

While the target for in vitro SIN inhibition is clear, how SIN inhibits viral replication in cells was less certain. Previous studies on SAM analogues, including SIN, have shown their potential to inhibit viral replication in cell culture (18, 41). However, the host SAH hydrolase, which catalyzes the hydrolysis of SAH to adenosine and L-homocysteine, will also serve as a target of SIN inhibition (14). Inhibition of SAH hydrolase function would perturb the intracellular ratio of SAM to SAH, which in turn would lead to a reduction of virus replication. The SIN^R mutants were selected for their growth properties in cells in the presence of SIN. Thus, it seems plausible that viral growth could be impacted by SIN targeting SAH hydrolase and/or the L protein.

The sequencing of the SIN^R mutants provides some insight into the intracellular target of SIN inhibition. All SIN^R mutants contained mutations in the *L* gene or key regulatory elements for L mRNA production, provided by the conserved *cis*-acting signals at the *G-L* gene junction. Three of the mutants, SIN^{R}1, -7, and -8, also each contained an *M* gene mutation. One strategy that might lead to SIN resistance is overproduction of the viral MTase. In the presence of SIN, all SIN^R mutants increased genomic RNA synthesis (Fig. 7B), and consistent with this, mRNA levels were typically increased (Fig. 7C). However, this was not universal, as SIN^{R}5 showed no increase in mRNA levels, and for SIN^{R}8 the increase was restricted to G and L mRNA (Fig. 7C). For mutants SIN^{R}1, -2, -4, -7, and -8 these changes were accompanied by an increase in levels of viral protein in the presence of SIN (Fig. 8B). Although increased viral gene expression is consistent with a viral protein being a target for SIN inhibition, upregulation of gene expression is also consistent with compensation for a perturbation of SAM and SAH levels in the cell, perhaps by allowing L to compete more effectively for SAM. In either event, these data suggest that a possible strategy for nsNS RNA viruses to acquire resistance to methylase inhibitors is to increase expression of the L protein MTase. Whether this increased expression is a direct response to SIN inhibiting the L MTase activities in cells or whether it reflects the fact that SIN inhibition of SAH hydrolase leads to increased SAH in the cell is not certain.

Amino acid changes in the L protein that permit the methylases to use SAM or release SAH more efficiently are a second potential means by which VSV might acquire resistance to SIN. Five mutants, SIN^{R}2, -4, -5, -7, and -8 contained amino acid substitutions in the L protein, and for the mutants SIN^{R}2, -4, -7, and -8 these changes were accompanied by a reduction in the sensitivity of the cap methylases to SIN in vitro (Fig. 5B and 6C). SIN^{R}2 contained an amino acid substitution within the MTase domain that might directly impact the ability of SIN to inhibit methylation. However, for SIN^{R}4, -5, -7, and -8 the amino acid changes were present in CR II and III of the L protein, which are not known to play a direct role in cap methylation. In the absence of SIN, we observed less L protein for mutants 2, 5, 7, and 8 compared to rVSV (Fig. 8A). This suggested that these amino acid substitutions also affect L protein synthesis or stability, which could impact viral growth, gene expression, and SIN sensitivity.

Some SIN^R mutants contained amino acid substitutions in the M protein, including the D55G substitution found for SIN^{R}1 and -8 and the M51R substitution for SIN^{R}7. Amino acid residues 51 and 55 reside within a nuclear localization signal for M that spans amino acids 47 to 57 (20, 39). Moreover, a well-characterized temperature-sensitive mutant of VSV (*ts*O82) contains the M51R substitution, which results in defects in the nuclear localization of M (20, 39), host cell

shutoff (3, 4), and induction of apoptosis (28). However, it seems unlikely that the *M* gene mutation is solely responsible for the phenotype of the SIN^R1 virus, which also contains an additional mutation in the *G-L* gene junction that expands the U tract of the *G* gene end from seven to eight residues. SIN^R3 contains only this latter alteration, and the phenotypic properties of this mutant are similar to those of SIN^R1. Nevertheless, it would be interesting to determine whether the altered M proteins are defective in nuclear localization and host cell shutoff.

Multiple regions of L protein impact mRNA cap methylation. Previously, CR VI of VSV and Sendai virus (SeV) L proteins was shown to function in mRNA cap methylation (22, 30, 31, 36). In addition, mutants of VSV that contain amino acid substitutions in a nonconserved region of the L protein adjacent to CR VI were found to be defective in mRNA methylation (21). In the present report we define amino acid substitutions in CR II/III and VI that affect methylation. The finding that the amino acid substitution in CR VI, K1749T, impacts cap methylation was not surprising based on the structure predictions of CR VI of mononegavirus L proteins (10, 19). While this specific residue is not conserved among nsNS RNA virus L proteins, it is predicted to occupy a position close to the SAM binding site of CR VI. It seems plausible that this substitution could directly impede SIN binding to the SAM binding site or could impact SAM binding or SAH release and thus lead to the this mutant having a growth advantage in the presence of SIN.

In contrast, it seems unlikely that CR II/III directly participates in the MTase activity; CR III is the core polymerase, and the primary sequence of region II does not resemble any known methylases (40). Rather, we propose that these amino acid substitutions indirectly impact CR VI, inhibiting its demonstrated activity as the viral mRNA cap methylase. Previous mutational analysis of the *L* gene of SeV that substituted clusters of residues within L demonstrated that amino acid alterations in CR II abolished all RNA synthesis (45). This was consistent with prior work that suggested that this region of L may be involved in template binding (34). The substitutions in CR II of L identified in this study were outside the region investigated for SeV L and at positions that are not conserved among nsNS RNA viruses. The suggestion that substitutions in CR II/III are indirectly impacting the methylation activity of CR VI is also consistent with the observation that substitutions in nonconserved regions of L protein can lead to defects in mRNA cap methylation (21). We interpret these data as illustrating that the global architecture of L protein can impact the mRNA cap-methylating enzymes. Previous work with the paramyxovirus measles virus demonstrated that the entire sequence of enhanced green fluorescent protein could be inserted into a "hinge" region between CR V and CR VI of the L protein (16). The resulting polymerase showed an approximately twofold reduction in gene expression as assessed by reporter gene activity, consistent with this recombinant virus containing modified *L* gene replicated with delayed kinetics compared to the wild-type virus. It would be of significant interest to evaluate the effect of this insertion on mRNA synthesis and cap methylation.

Mutations to conserved *cis*-acting signals at the G-L gene junction. Four of the SIN^R mutants contained mutations at the *G-L* gene junction. Among these were C4728A, which altered the conserved *L* gene start sequence from UUGUC to UUGUA in SIN^R6. This mutant showed a modest (approximately 15%) reduction in G-N-7 methylation. No other sequence changes were detected in the viral genome, which suggests that this reflects a specific defect in methylation of the L mRNA only. Under the in vitro synthesis conditions used, each of the VSV mRNAs was generated (Fig. 5C), and previous work with SeV demonstrated that small RNAs that correspond in sequence to the 5′ ends of the SeV mRNAs were methylated at position G-N-7 (36). We suggest that there may be a specific sequence requirement for cap methylation and that substitution C5A of the conserved gene start sequence inhibits this methylation. Experiments to evaluate the role of this sequence in each step of mRNA cap formation are under way.

Three of the SIN^R mutants, SIN^R1 to -3, expanded the U7 tract found at the *G* gene end to U8. This U tract provides the template on which polymerase stutters to generate the polyadenylate tail (7, 8, 26) and plays a second role in signaling efficient transcription of the downstream gene (24). Using genomic analogs of VSV, the presence of a U8 tract was shown to have a negligible effect on termination and polyadenylation of the upstream gene (9) or efficient transcription of the downstream gene (24). While the effect of expanding the U7 tract to U8 on viral gene expression has not been previously described, SIN^R3 contains only this mutation and produced elevated levels of each of the viral RNAs in cells (Fig. 7). We speculate that this mutation leads to an increase in L expression that subsequently enhances all mRNA synthesis.

Prospects for inhibiting nsNS RNA virus methylases. In the present study, we show that the methylase activities of VSV are direct targets in vitro for inhibition by SIN, a known potent methylase inhibitor. We further show that SIN inhibits viral growth in cell culture. The experiments described here show that the virus can acquire resistance to SIN inhibition perhaps by upregulating gene expression in cells, and that such SIN^R mutants were readily isolated following four passages of VSV. However, the resistant mutants showed a reduction in viral growth as judged by their plaque diameters. While the mutants have a selective advantage in the presence of SIN, their plaque morphologies suggest that they are less fit than their wild-type parent, rVSV.

In summary, we show that a known potent MTase inhibitor can directly inhibit the MTase activities of VSV and that the resistance to such an inhibitor is acquired by accumulating mutations that are frequently associated with increased gene expression in the presence of the inhibitor. We also show that substitutions in multiple regions of L can impact viral mRNA methylation in vitro. The MTase activities of nsNS RNA viruses are considered attractive targets for antiviral intervention, and these findings are relevant to this objective because they demonstrate that such inhibitors can directly target the MTase activities of VSV.

ACKNOWLEDGMENTS

We thank Steve Lory for suggesting the use of SIN and members of the Whelan laboratory for their critical review of the manuscript.

This work was supported by grant AI059371 from the National Institutes of Health to S.P.J.W.

REFERENCES

1. **Abraham, G., and A. K. Banerjee.** 1976. Sequential transcription of the genes of vesicular stomatitis virus. Proc. Natl. Acad. Sci. USA **73:**1504–1508.
2. **Abraham, G., D. P. Rhodes, and A. K. Banerjee.** 1975. The 5′ terminal structure of the methylated mRNA synthesized in vitro by vesicular stomatitis virus. Cell **5:**51–58.
3. **Ahmed, M., and D. S. Lyles.** 1997. Identification of a consensus mutation in M protein of vesicular stomatitis virus from persistently infected cells that affects inhibition of host-directed gene expression. Virology **237:**378–388.
4. **Ahmed, M., M. O. McKenzie, S. Puckett, M. Hojnacki, L. Poliquin, and D. S. Lyles.** 2003. Ability of the matrix protein of vesicular stomatitis virus to suppress beta interferon gene expression is genetically correlated with the inhibition of host RNA and protein synthesis. J. Virol. **77:**4646–4657.
5. **Ball, L. A., and C. N. White.** 1976. Order of transcription of genes of vesicular stomatitis virus. Proc. Natl. Acad. Sci. USA **73:**442–446.
6. **Baltimore, D., A. S. Huang, and M. Stampfer.** 1970. Ribonucleic acid synthesis of vesicular stomatitis virus, II. An RNA polymerase in the virion. Proc. Natl. Acad. Sci. USA **66:**572–576.
7. **Barr, J. N., and G. W. Wertz.** 2001. Polymerase slippage at vesicular stomatitis virus gene junctions to generate poly(A) is regulated by the upstream 3′-AUAC-5′ tetranucleotide: implications for the mechanism of transcription termination. J. Virol. **75:**6901–6913.
8. **Barr, J. N., S. P. Whelan, and G. W. Wertz.** 1997. *cis*-Acting signals involved in termination of vesicular stomatitis virus mRNA synthesis include the conserved AUAC and the U7 signal for polyadenylation. J. Virol. **71:**8718–8725.
9. **Barr, J. N., S. P. Whelan, and G. W. Wertz.** 1997. Role of the intergenic dinucleotide in vesicular stomatitis virus RNA transcription. J. Virol. **71:** 1794–1801.
10. **Bujnicki, J. M., and L. Rychlewski.** 2002. In silico identification, structure prediction and phylogenetic analysis of the 2′-O-ribose (cap 1) methyltransferase domain in the large structural protein of ssRNA negative-strand viruses. Protein Eng. **15:**101–108.
11. **Chuang, J. L., and J. Perrault.** 1997. Initiation of vesicular stomatitis virus mutant polR1 transcription internally at the N gene in vitro. J. Virol. **71:** 1466–1475.
12. **Colonno, R. J., and H. O. Stone.** 1976. Newcastle disease virus mRNA lacks 2′-O-methylated nucleotides. Nature **261:**611–614.
13. **De Clercq, E.** 2004. Antivirals and antiviral strategies. Nat. Rev. Microbiol. **2:**704–720.
14. **De Clercq, E.** 1987. S-Adenosylhomocysteine hydrolase inhibitors as broad-spectrum antiviral agents. Biochem. Pharmacol. **36:**2567–2575.
15. **De Clercq, E., and J. A. Montgomery.** 1983. Broad-spectrum antiviral activity of the carbocyclic analog of 3-deazaadenosine. Antiviral Res. **3:**17–24.
16. **Duprex, W. P., F. M. Collins, and B. K. Rima.** 2002. Modulating the function of the measles virus RNA-dependent RNA polymerase by insertion of green fluorescent protein into the open reading frame. J. Virol. **76:**7322–7328.
17. **Emerson, S. U., and Y. Yu.** 1975. Both NS and L proteins are required for in vitro RNA synthesis by vesicular stomatitis virus. J. Virol. **15:**1348–1356.
18. **Fabianowska-Majewska, K., J. A. Duley, and H. A. Simmonds.** 1994. Effects of novel anti-viral adenosine analogues on the activity of S-adenosylhomocysteine hydrolase from human liver. Biochem. Pharmacol. **48:**897–903.
19. **Ferron, F., S. Longhi, B. Henrissat, and B. Canard.** 2002. Viral RNA-polymerases—a predicted 2′-O-ribose methyltransferase domain shared by all *Mononegavirales*. Trends Biochem. Sci. **27:**222–224.
20. **Glodowski, D. R., J. M. Petersen, and J. E. Dahlberg.** 2002. Complex nuclear localization signals in the matrix protein of vesicular stomatitis virus. J. Biol. Chem. **277:**46864–46870.
21. **Grdzelishvili, V. Z., S. Smallwood, D. Tower, R. L. Hall, D. M. Hunt, and S. A. Moyer.** 2006. Identification of a new region in the vesicular stomatitis virus L polymerase protein which is essential for mRNA cap methylation. Virology **350:**394–405.
22. **Grdzelishvili, V. Z., S. Smallwood, D. Tower, R. L. Hall, D. M. Hunt, and S. A. Moyer.** 2005. A single amino acid change in the L-polymerase protein of vesicular stomatitis virus completely abolishes viral mRNA cap methylation. J. Virol. **79:**7327–7337.
23. **Hercyk, N., S. M. Horikami, and S. A. Moyer.** 1988. The vesicular stomatitis virus L protein possesses the mRNA methyltransferase activities. Virology **163:**222–225.
24. **Hinzman, E. E., J. N. Barr, and G. W. Wertz.** 2002. Identification of an upstream sequence element required for vesicular stomatitis virus mRNA transcription. J. Virol. **76:**7632–7641.
25. **Hunt, D. M.** 1983. Vesicular stomatitis virus mutant with altered polyadenylic acid polymerase activity in vitro. J. Virol. **46:**788–799.
26. **Hwang, L. N., N. Englund, and A. K. Pattnaik.** 1998. Polyadenylation of vesicular stomatitis virus mRNA dictates efficient transcription termination at the intercistronic gene junctions. J. Virol. **72:**1805–1813.
27. **Iverson, L. E., and J. K. Rose.** 1981. Localized attenuation and discontinuous synthesis during vesicular stomatitis virus transcription. Cell **23:**477–484.
28. **Kopecky, S. A., M. C. Willingham, and D. S. Lyles.** 2001. Matrix protein and another viral component contribute to induction of apoptosis in cells infected with vesicular stomatitis virus. J. Virol. **75:**12169–12181.
29. **Lehrach, H., D. Diamond, J. M. Wozney, and H. Boedtker.** 1977. RNA molecular weight determinations by gel electrophoresis under denaturing conditions, a critical reexamination. Biochemistry **16:**4743–4751.
30. **Li, J., E. C. Fontaine-Rodriguez, and S. P. Whelan.** 2005. Amino acid residues within conserved domain VI of the vesicular stomatitis virus large polymerase protein essential for mRNA cap methyltransferase activity. J. Virol. **79:**13373–13384.
31. **Li, J., J. T. Wang, and S. P. Whelan.** 2006. A unique strategy for mRNA cap methylation used by vesicular stomatitis virus. Proc. Natl. Acad. Sci. USA **103:**8493–8498.
32. **Li, T., and A. K. Pattnaik.** 1999. Overlapping signals for transcription and replication at the 3′ terminus of the vesicular stomatitis virus genome. J. Virol. **73:**444–452.
33. **Moyer, S. A., G. Abraham, R. Adler, and A. K. Banerjee.** 1975. Methylated and blocked 5′ termini in vesicular stomatitis virus in vivo mRNAs. Cell **5:**59–67.
34. **Muller, R., O. Poch, M. Delarue, D. H. Bishop, and M. Bouloy.** 1994. Rift Valley fever virus L segment: correction of the sequence and possible functional role of newly identified regions conserved in RNA-dependent polymerases. J. Gen. Virol. **75:**1345–1352.
35. **Nolan, L. L.** 1987. Molecular target of the antileishmanial action of sinefungin. Antimicrob. Agents Chemother. **31:**1542–1548.
36. **Ogino, T., M. Kobayashi, M. Iwama, and K. Mizumoto.** 2005. Sendai virus RNA-dependent RNA polymerase L protein catalyzes cap methylation of virus-specific mRNA. J. Biol. Chem. **280:**4429–4435.
37. **Paolantonacci, P., F. Lawrence, L. L. Nolan, and M. Robert-Gero.** 1987. Inhibition of leishmanial DNA synthesis by sinefungin. Biochem. Pharmacol. **36:**2813–2820.
38. **Pattnaik, A. K., and G. W. Wertz.** 1990. Replication and amplification of defective interfering particle RNAs of vesicular stomatitis virus in cells expressing viral proteins from vectors containing cloned cDNAs. J. Virol. **64:**2948–2957.
39. **Petersen, J. M., L. S. Her, and J. E. Dahlberg.** 2001. Multiple vesiculoviral matrix proteins inhibit both nuclear export and import. Proc. Natl. Acad. Sci. USA **98:**8590–8595.
40. **Poch, O., B. M. Blumberg, L. Bougueleret, and N. Tordo.** 1990. Sequence comparison of five polymerases (L proteins) of unsegmented negative-strand RNA viruses: theoretical assignment of functional domains. J Gen. Virol. **71:**1153–1162.
41. **Pugh, C. S., R. T. Borchardt, and H. O. Stone.** 1978. Sinefungin, a potent inhibitor of virion mRNA(guanine-7-)-methyltransferase, mRNA(nucleoside-2′-)-methyltransferase, and viral multiplication. J. Biol. Chem. **253:**4075–4077.
42. **Schluckebier, G., M. Kozak, N. Bleimling, E. Weinhold, and W. Saenger.** 1997. Differential binding of S-adenosylmethionine S-adenosylhomocysteine and sinefungin to the adenine-specific DNA methyltransferase M.*Taq*I. J. Mol. Biol. **265:**56–67.
43. **Schluckebier, G., P. Zhong, K. D. Stewart, T. J. Kavanaugh, and C. Abad-Zapatero.** 1999. The 2.2 Å structure of the rRNA methyltransferase ErmC′ and its complexes with cofactor and cofactor analogs: implications for the reaction mechanism. J. Mol. Biol. **289:**277–291.
44. **Sleat, D. E., and A. K. Banerjee.** 1993. Transcriptional activity and mutational analysis of recombinant vesicular stomatitis virus RNA polymerase. J. Virol. **67:**1334–1339.
45. **Smallwood, S., C. D. Easson, J. A. Feller, S. M. Horikami, and S. A. Moyer.** 1999. Mutations in conserved domain II of the large (L) subunit of the Sendai virus RNA polymerase abolish RNA synthesis. Virology **262:**375–383.
46. **Szilagyi, J. F., and L. Uryvayev.** 1973. Isolation of an infectious ribonucleoprotein from vesicular stomatitis virus containing an active RNA transcriptase. J. Virol. **11:**279–286.
47. **Testa, D., and A. K. Banerjee.** 1977. Two methyltransferase activities in the purified virions of vesicular stomatitis virus. J. Virol. **24:**786–793.
48. **Villarreal, L. P., M. Breindl, and J. J. Holland.** 1976. Determination of molar ratios of vesicular stomatitis virus induced RNA species in BHK21 cells. Biochemistry **15:**1663–1667.
49. **Wertz, G. W., S. Whelan, A. LeGrone, and L. A. Ball.** 1994. Extent of terminal complementarity modulates the balance between transcription and replication of vesicular stomatitis virus RNA. Proc. Natl. Acad. Sci. USA **91:**8587–8591.
50. **Whelan, S. P., and G. W. Wertz.** 1999. Regulation of RNA synthesis by the genomic termini of vesicular stomatitis virus: identification of distinct sequences essential for transcription but not replication. J. Virol. **73:**297–306.
51. **Whelan, S. P., and G. W. Wertz.** 2002. Transcription and replication initiate at separate sites on the vesicular stomatitis virus genome. Proc. Natl. Acad. Sci. USA **99:**9178–9183.
52. **Zheng, S., S. Hausmann, Q. Liu, A. Ghosh, B. Schwer, C. D. Lima, and S. Shuman.** 2006. Mutational analysis of *Encephalitozoon cuniculi* mRNA cap (guanine-N7) methyltransferase, structure of the enzyme bound to sinefungin, and evidence that cap methyltransferase is the target of sinefungin's antifungal activity. J. Biol. Chem. **47:**35904–35913.